J. Fluid Mech. (1976), *vol.* 78, *part* 3, *pp.* 459–480
Printed in Great Britain

A stationary oblique breaking wave for laboratory testing of surfboards

By H. G. HORNUNG AND P. KILLEN

Department of Physics, School of General Studies, Australian National University, Canberra

(Received 7 May 1976)

A surface gravity wave obliquely incident on a sloping beach is broken near the beach and has a smooth surface further out. Viewed in the frame of reference of the transition from the smooth to the broken part, the flow is steady, and the wave is oblique to the free stream. By placing a suitably shaped obstacle in a flume operated at high Froude number, such a wave can be generated. Experiments in which a wave of 18 cm height was generated are described and the wave shape and some of its characteristics presented. In particular, the dividing stream surface separating that part of the flow which curls over into the break from the part that flows smoothly over the obstacle is discussed.

Model surfboards can ride this wave unsupported, provided the correctly scaled weight loads them at the right centre-of-mass position. This makes it possible to determine the forces on the board without a balance. A comparison of the measured forces with estimates, particularly of the drag, indicate that viscous and surface-tension phenomena introduce only small scale effects in the Froude number modelling. While the results are not sufficiently accurate to draw definite conclusions about the effects of surfboard shape, they indicate clearly that surfboard flows may be modelled with quantitative success in the laboratory.

1. Introduction

When a water wave is obliquely incident on a sloping beach, the portion of it closest to the beach is broken, while that furthest from the beach has a smooth surface. The transition from the smooth to the broken part of the wave occurs continuously over a region spanning a few wave heights. The wave face reaches its maximum slope in this transition region, which is therefore the part of the wave most suitable for the purposes of the surfboard rider, who uses the wave face much like a skier uses a mountain. Because he continually moves with the point at which the wave is just breaking, that is with the point at which the water depth reaches a certain value, the path of the surfboard rider is parallel to the bottom contour, and his average velocity is that of the intersection of the wave with the bottom contour, so that he moves faster than the propagation speed of the wave even if his velocity is constant.

Although some excellent films have been made of surfboard riders on moving waves, the detailed information obtainable from these is very limited and, because

of the obvious difficulty of conditions at a beach, very expensive. For the case of a surfboard rider with constant velocity, however, the problem can be transformed into a steady one by observing from the frame of reference of the rider, that is, of the region of transition from smooth to broken wave. Hence, if a stationary wave with the necessary characteristics can be generated in the laboratory, it should be possible to study the steady motion of a surfboard in its own frame of reference.

It is clear that the experiment has to be made in a stream of water with a velocity of equivalent magnitude and opposite direction to that of the surfboard in the real situation, in which the water at a large distance from the board is stationary. Such streams of water are available in laboratories in the form of water channels or flumes, the typical size of which is usually 1 m across the flow direction. Since in the real situation the transition from smooth to broken wave occurs typically over a distance of 10 m, the laboratory wave must be scaled down. It must also be an oblique wave, that is, its direction of propagation relative to the free stream must have a component across the flume and the wave must be breaking at its downstream end while being smooth at its upstream end.

Both the problem of the wave and that of a planing board have been treated in simple cases before. Thus, experiments and numerical calculations of waves normally incident on a sloping beach have been made (see Stoker 1957, § 10.10). Also Wagner (1932) calculated the flow under a planing hull by the methods of incompressible flow wing theory. Others after him have extended and refined his approach (see, for example, Sedov 1965, and, for further references, Wehausen & Laitone 1960). However, the situation with both the wave and the surfboard is, in the present problem, so far from the simplifying idealizations necessary to make the problems accessible to theory that this previous work is only useful in a qualitative way. The approach in the present work is therefore essentially empirical.

The first aim of the present work was to generate a stationary scale model of the transition from the smooth to broken wave obliquely across a flume in such a way that the surface shape of the wave is as nearly geometrically similar to an ideal wave in the real surfing situation as possible. The second aim was to build models of surfboards to the same scale, suitably weighted to produce a situation dynamically similar to the constant-velocity surfboard, and to study the variation of the steady-state characteristics and the stability of boards with simple shape variations. In effect, the feasibility of testing scale models of surfboards in a flume and the inevitable scale effects associated with the modelling were to be examined.

2. The flume

The flume in which the present experiments were made is 0·91 m wide, and 9·1 m long. The maximum volume flow rate is 0·17 $m^3 s^{-1}$. The water is pumped from an underground tank of 50 m^3 capacity through a pipe of 30 cm diameter into a header tank of 9 m^3 capacity from which it flows through a bank of closely packed polythene tubes (3·8 cm diameter, 45 cm long) into the flume. The cross-

sectional area of the tube bank is approximately 1 m^2. In the present experiments the tube bank is followed by a smooth, broad-crested weir made of aluminium sheet, formed over a wooden support structure. On the downstream side the weir blends smoothly (with continuous slope) into the wooden floor of the flow which is also raised above the permanent floor of the flume by a wooden structure. The side walls of the flume are made of glass between aluminium frames such that the inside is flush along the full length. The top is open between the frames. The slope of the flume is continuously adjustable from 0 to 2·5° from the horizontal, by a hydraulically operated ramp device.

3. The wave

3.1. *Shape parameters*

As a smooth ocean wave travels shoreward at normal incidence, the depth of the water decreases. The constraint imposed on the periodic motion of the particles in the wave by the rising ocean floor causes the wave face to steepen to form a cusped crest which eventually breaks into an entrailed plume on the wave face. The shape of the wave at this point is of interest and depends mainly on the slope of the beach. If the depth decreases sufficiently rapidly the top of the wave plunges forward bodily without forming a plume and strikes the surface somewhere on the wave face (see Stoker 1957, § 10.10). A suitable measure of the wave shape is the ratio S of the throw b of the curl to the wave height h, as defined in figure 1. Large values of S are preferred by surfers because such waves have steep faces and hence can produce higher surfboard speeds, as well as supplying the excitement and danger associated with surfing inside the tube.

If the wave is obliquely incident on the beach, a second parameter necessary to describe the wave shape is the angle γ made by the wave front and the beach contours. While a wave which is normally incident on the beach is plane but unsteady, the obliquely incident wave is three-dimensional and steady, if viewed from co-ordinates fixed in that part of the wave which is just breaking. The speed of this transition region, or the break speed v_b, is directed parallel to the beach contour and is related to the phase speed of the wave v_w by

$$v_b = v_w/\sin\gamma. \tag{1}$$

3.2. *The obstacle*

The three-dimensional steady wave obliquely incident on the beach is analogous to the two-dimensional unsteady wave with normal incidence, the co-ordinate along the wave front in the former case corresponding to time in the latter. Thus, the dotted line in figure 1 representing the wave shape at some time before breaking would be observed in the oblique case on that part of the wave which is further from the beach than the break.

In order to simulate the oblique wave in the flume it is necessary to accelerate the water to a speed corresponding to the value of v_b associated with the wave. Since this is directly related to the wave speed v_w the free-stream speed is governed by the size of the wave. This in turn is limited by the size of the facility, and in

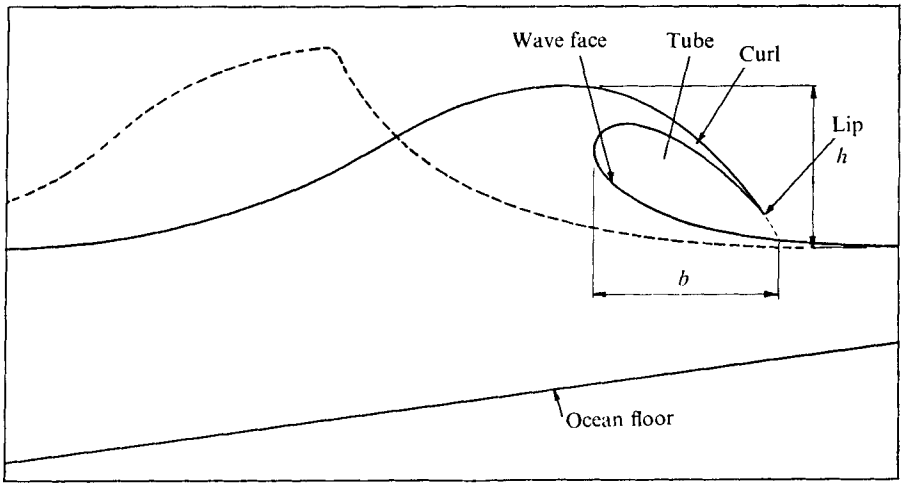

FIGURE 1. Two-dimensional unsteady breaking wave.
- - - -, surface at earlier time.

the present experiment the wave height h is restricted to approximately 20 cm. With an angle γ of around 45°, the free-stream water speed must therefore be approximately $2\,\mathrm{m\,s^{-1}}$ for a wave of this size to be stationary. The water depth in the free stream is less than 20 cm, and the free stream is in a condition of rapid (or supercritical) flow. The acceleration from tranquil to rapid flow is achieved by the reduction in water height through the broad-crested weir, which is analogous to a Laval nozzle in gas flow. The speed is maintained constant after the accelerating weir and subsequent steep portion of the floor, by a constant slope of the floor (1° 20′) which is chosen to compensate approximately for the losses due to skin friction at the floor and walls.

In the case of the obliquely incident ocean wave, energy is continually fed into the break by the arrival of the unbroken wave. This energy has to be supplied in the case of the laboratory wave by the resistance to the flow of an obstacle of some form suitable to generate the desired wave shape. Although analytic techniques exist (see Lamb 1932) they are difficult in this three-dimensional case, and the process by which the shape of the obstacle is determined in the present experiment is quite empirical, the only guideline being the analogy between the oblique gravity wave in supercritical water flow and an oblique shock wave in supersonic gas flow. Accordingly, the material chosen for the obstacle is plasticine, so that its shape can be modified to change the resulting wave shape by trial and error.

In plane supersonic gas flow, a stationary oblique wave may be generated by deflecting the flow with a wedge. The character of the wave may be made to vary along its length, from an isentropic compression near the tip of the wedge to a shock wave further along, by making the wedge surface concave (see figure 2). If an experiment like this is performed in a supersonic wind tunnel, it is advisable to raise the wedge off the tunnel floor A to avoid separation of the tunnel-wall boundary layer. Similarly, the shock wave incident on the tunnel

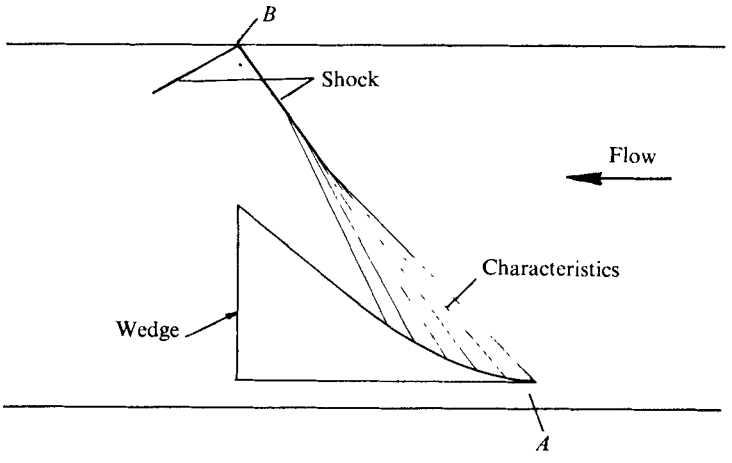

FIGURE 2. Isentropic compression wave steepening into a shock in supersonic gas flow. *A*, channel to avoid boundary-layer separation; *B*, shock-induced separation may cause choking of the flow.

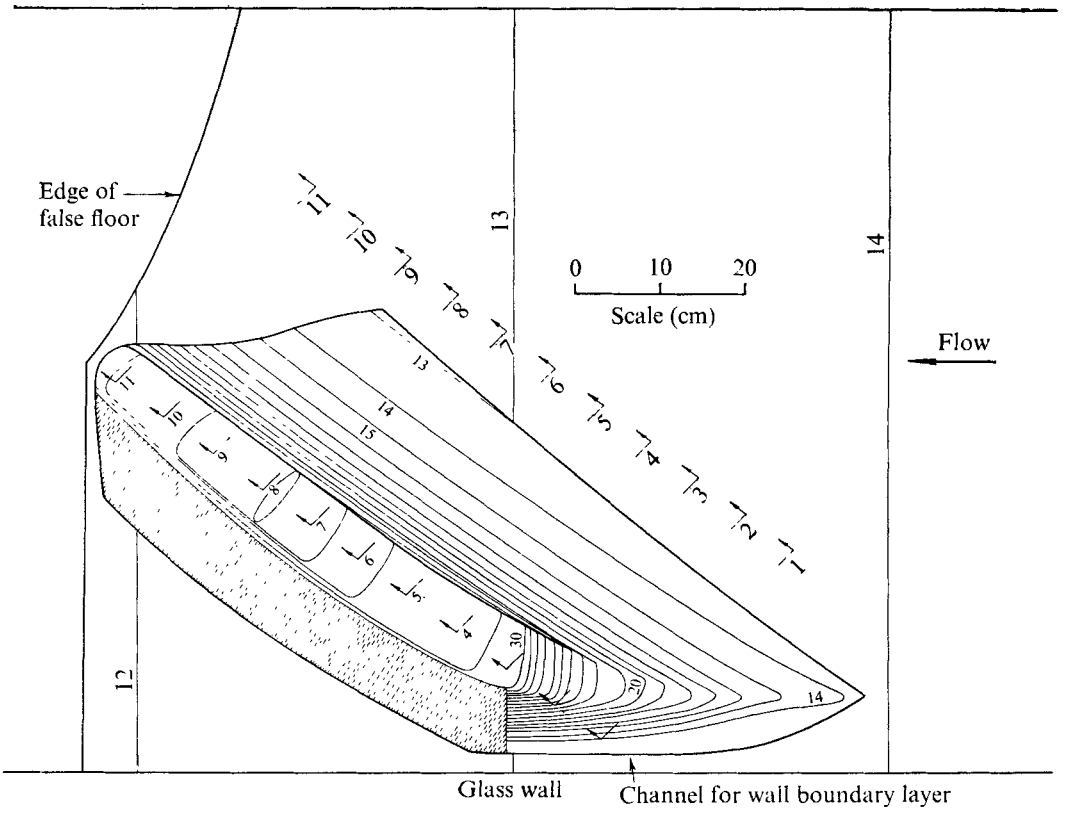

FIGURE 3. Contour map of the obstacle. The numbers on the contours indicate vertical height in cm. The numbered arrows show the location of the sections in figure 5.

roof B may cause the boundary layer to separate there and result in 'choking' of the entire flow.

In the present experiments the procedure of simulating an ocean wave is necessarily approximate, because no acccurate measurements or adequate theories are available to describe the desirable wave. The criteria for judging whether or not the wave produced has the right characteristics are comparisons of the surface shape with photographs of ocean waves, and comparisons with experience gained in riding ocean waves. There is, of course, some leeway in these criteria because a considerable variety of wave shapes can be ridden.

Some simple rules of behaviour emerge from experiments with a straight obstacle: reducing the angle of incidence of the obstacle reduces the wave angle γ as well as S. At constant γ, S is most easily controlled by varying the cross-sectional shape of the obstacle face. It is essential to terminate the obstacle about half way across the flume to prevent choking of the flow by the wave. In fact even that leaves too small a gap, and the wave builds up into a normal hydraulic jump which moves to a stable position further upstream. To prevent this choking, the false floor mentioned in § 2 is terminated immediately after the trailing end of the obstacle so that the water spills down over a step of about 30 cm height.

The final form of the obstacle is shown in figure 3 in the form of a contour map. It can be seen that only a slight curvature has been built into the contours on the obstacle face and that the tip builds up gradually in a backward sweep, leaving a space for the channel-wall boundary layer to be washed past outside the region of interest. The end of the false floor is also indicated in the figure.

3.3. *The model wave*

A photograph of the type of ocean wave we wished to reproduce in the flume is shown in figure 4(*a*) (plate 1); figure 4(*b*) (plate 1) shows a similar view of the model wave produced when a stream at 2·24 m s^{-1} and 7·8 cm free-stream depth flows over the obstacle of figure 3. It can be seen that quite good surface similarity may be achieved, although one of the differences between the two waves is evident in the photographs. This is due to the relatively greater importance of surface tension in the model wave, which manifests itself in an apparently more rounded lip on the curl. The radius of curvature of the lip is, of course, approximately the same in both waves, the sharper appearance of the ocean wave being due to its larger size. As can be seen by the nature of the broken part of the wave in figure 4(*b*) the photograph is made by a short time exposure (0·0003 s). The apparent thickening of the curl just before it strikes the wave face is a transient effect, a broad splash of liquid leaving the curl in a downward and inward direction. The size of this splash is indicative of the magnitude of the fluctuations in the free stream, which amounts to approximately $\pm 5\%$ of the free-stream depth.

While the wave cannot be compared with the ocean wave in greater detail because of the lack of data on the latter, a thorough measurement of the laboratory wave is possible and indeed necessary in order to make the experiments meaningful.

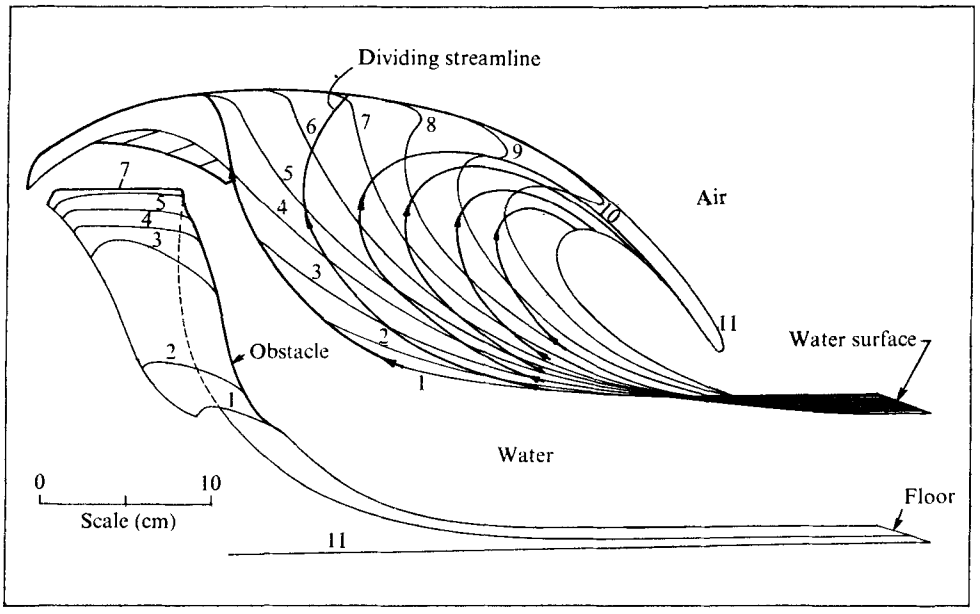

FIGURE 5. Side view of the wave, taken at the sections shown in figure 3 with section numbers marked. Heavy lines with arrowheads show surface streamlines.

To do this, the mean position of the surface and the shape of surface streamlines, made visible by injecting dye, are measured by a three-dimensional traversing device. The free-surface shape is shown in figure 5 in the form of 11 vertical sections through the wave, taken at the positions marked in figure 3. Also indicated in the diagram is the position and shape of the obstacle in the same sectional representation. The viewing direction is tangential to the downstream part of the contours on the obstacle face. Thus one sees the free-stream surface from underneath. The light lines in figure 5 represent the free surface, the numbers indicating the evenly spaced sections progressing in a downstream direction along the wave. The co-ordinate in this direction is expected to be analogous to time in the two-dimensional unsteady case of a wave normally incident on a sloping beach. This analogy is illustrated by figure 5, in which section number 4 is still like a smooth wave, and a continuous progression leads through the sections to 11, in which the curl is about to strike the wave face.

The temporal mean position of surface streamlines is also shown in figure 5 in the form of heavier lines with arrowheads. Since the flow is steady, the free surface is a stream surface and streamlines are tangential to it everywhere. This is not true, of course, for submerged stream surfaces, which may, in special cases, meet the liquid surface at a finite angle. An example is a dividing stream surface, the intersection of which in the liquid surface is a dividing surface streamline.

Such a dividing stream surface occurs in the oblique wave, and its concomitant dividing surface streamline is shown in figure 5. The streamlines to the left and below the dividing stream surface pass over the obstacle smoothly, without

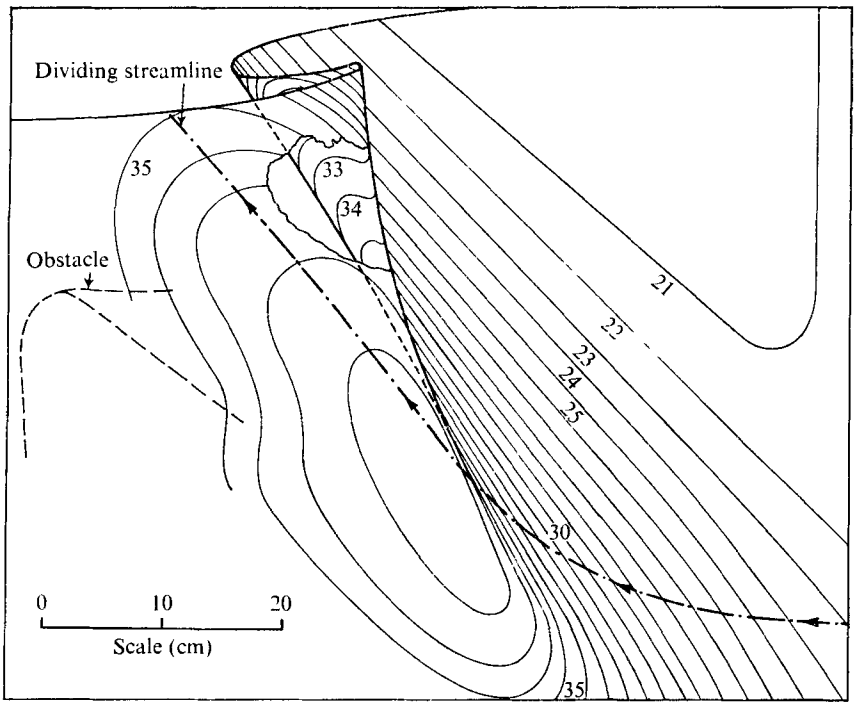

FIGURE 6. Contour map of the water surface. The numbers indicate vertical height in cm. The contours on the roof of the tube are shown in the cut-out. The streamline shown is the dividing surface streamline.

being involved in the broken part of the wave. The fluid on streamlines above and to the right of it on the other hand diverges strongly into the curl and passes into the violently turbulent and frothy break, from which it emerges and moves in a direction approximately parallel to the obstacle as in supersonic gas flow over a wedge. The free-stream fluctuations are actually helpful in detecting the dividing streamline, since, if the dye is injected in the right position, the slightly jagged streamline broadens dramatically into a divergent smear just as it reaches the crest of the wave. The dividing surface streamline is shown also in the contour map of the liquid surface (figure 6) in which the locus of the vertical tangent to the surface inside the tube is marked as a heavy dotted line and the lip of the curl is indicated by a heavy solid line. The light lines indicate contours, which are also shown underneath the curl in a small cut-out. The light dotted lines show the outline of the obstacle to locate the diagram relative to figures 3 and 5.

The analogy between a compression wave in supersonic gas flow and a gravity wave in shallow water is emphasized by plotting the free surface in a contour map such as figure 6. This is because the height contours of the free surface are characteristic curves and correspond to the Mach waves of the gas-flow case. Thus, the coalescing of characteristics of the same family into a shock wave manifests itself in the water wave as a steepening to a vertical face. The analogy

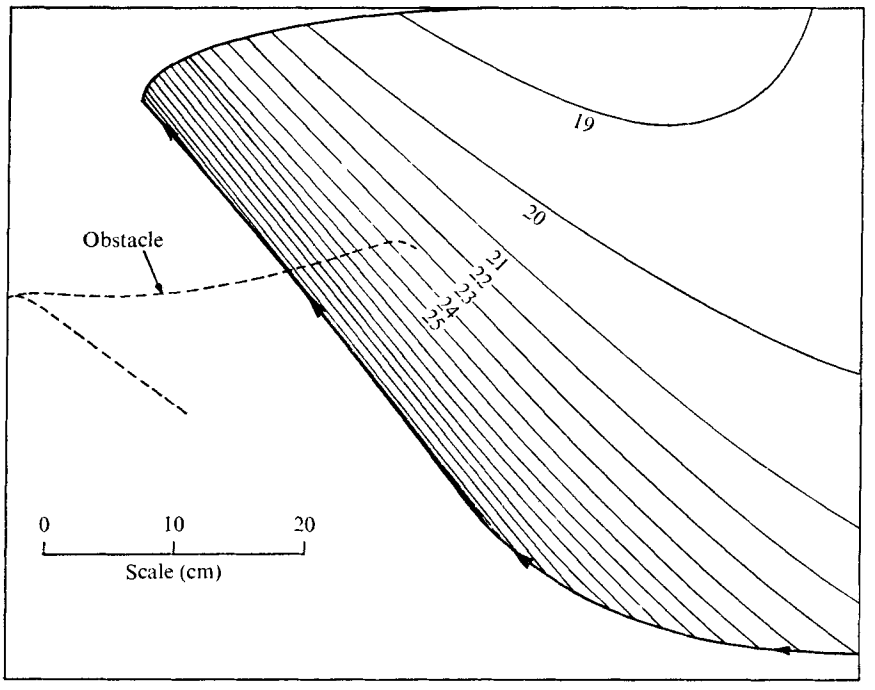

FIGURE 7. Contour map of the dividing stream surface, whose trace in the liquid surface is the dividing surface streamline.

fails just there, however, as the height contours may intersect in the region of the curl, while this would not be possible in a gas shock. It should be remembered, however, that the scale of the shock thickness is usually small in gasdynamic problems while the thickness of the hydraulic jump in the present problem is of the same order as the overall scale of the flow. The jump–shock analogy may therefore be expected to be more useful in a situation where the wave thickness is small compared with the overall scale of the problem.

Figure 7 shows the contours of the dividing stream surface. These are obtained by varying the depth at which dye is injected in the free stream until the streamline divides, measuring the shape of the streamline with a probe and repeating the process at several stations across the flume. Because of the broadening of the surface dividing streamline near its downstream end, the mean position of the dividing stream surface becomes more difficult to determine in the vicinity of the dividing surface streamline. Consequently the position of this part of the surface can only be measured repeatably to an accuracy of $\pm$ 1·5 cm. Elsewhere (in figures 5, 6 and 7) the accuracy is limited by the fluctuations in the free stream to $\pm$ 0·3 cm. Measurements of a stream surface below the dividing stream surface and originating from 2 cm below the liquid surface in the free stream show that this surface is smooth despite the somewhat angular shape of the obstacle.

The part of the wave below and just upstream of the lip of the curl (see figure 6) is the region of the liquid surface of main interest to the surfboard rider, and

the detail of the slopes of the surface is required for the following sections. The overall properties of the wave are collected here for clarity:

$$\text{free-stream speed} = 2{\cdot}24\,\text{m s}^{-1},$$
$$\text{wave height } h = 18\,\text{cm},$$
$$\text{throw of curl } l = 8\,\text{cm},$$
$$\text{wave angle } \gamma = 48^\circ$$

(measured between free-stream direction and 25 cm contour).

Apart from the fact that the model wave is smaller than the ocean wave, so that surface-tension effects are more important, another difference between the two situations is that the relative velocity of the free stream and the floor is not zero in the model situation. This means that there is a boundary layer on the floor which may be sufficiently thick to affect the flow near the liquid surface and so to influence the flow around the fin of a surfboard. A boundary-layer traverse, made in the free stream at a station just upstream of the wave (2·5 m from the weir), shows that the 95 % thickness of the (turbulent) boundary layer is less than 3·5 cm, thus occupying less than the lower half of the flow.

4. The surfboard riding on the wave

4.1. *The modelling problem*

When a surfboard rides a wave in steady flow the force P exerted on it by the water may be expected to depend on the water density ρ, viscosity μ, surface tension σ, speed V relative to the board, the acceleration of gravity g, a length d characterizing the board size, the wave height h and the shapes of the wave and board. This relationship may be expressed in dimensionless form:

$$\frac{P}{\rho V^2 d^2} = f\left(\frac{V}{(dg)^{\frac{1}{2}}}, \frac{\rho V d}{\mu}, \frac{\sigma}{\rho g d^2}, \frac{d}{h}, S, \gamma, \text{board shape}\right), \tag{2}$$

or

$$C_P = f(F, R, W, d/h, S, \gamma, \text{board shape}), \tag{3}$$

where f defines the relationship (unknown until the problem is solved) between the force coefficient C_P, the Froude, Reynolds and Weber numbers F, R, W, the parameters S and γ and the board size and shape.

In a similar way, the wave-shape parameters γ and S are related to the obstacle shape, and to the Froude, Reynolds and Weber numbers, with h replacing d in F and W, and a length which characterizes the boundary-layer development on the flume floor replacing d in R. However, as has been pointed out in § 3, the boundary layer on the flume floor is thin enough in the present experiments for the Reynolds number to be unimportant in the case of the wave. The Weber number essentially affects only the sharpness of the lip, provided that h is much larger than 1 cm (on a scale of between 1 and 2 cm, gravity and surface-tension effects in water are equally important). Hence the wave modelling, keeping the Froude number constant, is not fraught unduly with scale effects

due to the difference between model and prototype Reynolds and Weber numbers in the present experiments. (No attempt was made to lower the surface tension of the water by using additives.)

The same may not be true of the surfboard modelling. The quantities $v_w/(hg)^{\frac{1}{2}}$, γ and S are the same for the model and prototype waves. Hence, if d/h as well as the liquid properties are the same for model and prototype, R and W are necessarily changed by the scaling. This is likely to be quite important in the present experiments because, for the model, R is in the laminar or transition region while the boundary layer on the prototype board is certainly turbulent. Since the model board is closer in size to the 1 cm scale of surface tension, the Weber number is relatively more important, both in the capillary waves and in regions of large surface curvature under the board. The modelling of surfboards riding a wave of approximately 20 cm height can therefore only be expected to be quantitatively successful if the forces due to surface tension and viscosity are unimportant compared with the total force on the board. However, by analogy with the results of subsonic wing theory, it may be expected that the scale effects significantly influence only the drag and not the lift force on the board.

4.2. *Main results of previous work*

In a classic treatment of the inviscid planing problem at infinite Froude number and zero Weber number, Wagner (1932) obtained solutions to a number of steady and unsteady planing problems, by showing first the correspondence between such flows and the flow on the pressure side of equivalent fully submerged wings. To the Kutta condition in the latter there corresponds, in the former, the requirement that the free surface has to leave the trailing edge of the planing board in the direction of the bottom surface of the board. The flow above the stagnation streamline is different in the two cases, the forward moving flow becoming a drag-producing splash in the direction of the planing board in the one case, while it flows over onto the suction side in the case of the wing, producing a drag-reducing low pressure on the leading edge.

As will be shown below, one of the cases treated by Wagner is particularly relevant to the surfboard flow. This is the unsteady, centrally similar problem of a two-dimensional semi-infinite flat plate entering the liquid surface obliquely, trailing edge first, while the plate is at incidence. The trailing edge is always parallel to the water surface, and all other angles to the horizontal are assumed small. Figure 8 shows the configuration and the deformed water surface. The similarity centre is the point where the trailing edge of the plate first strikes the liquid surface. The discontinuity of the tangential velocity at the liquid surface in the wake amounts to a vortex sheet, which rotates the free surface, raising it at the similarity centre and lowering it near the trailing edge. The flow is similar to that of an impulsively started wing, which leaves a starting vortex behind. Figure 8 also shows the splash formed at the leading edge of the wetted surface. The mid-point of the wetted surface, x_0 from the similarity centre, is of course not necessarily on the undisturbed waterline. To find its path and to determine the angle β it is necessary to find the shape of the deformed free surface

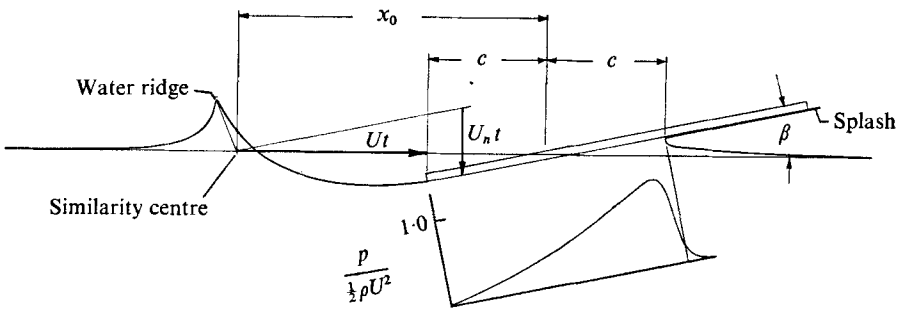

FIGURE 8. Wagner's unsteady centrally similar two-dimensional planing problem with schematic pressure distribution.

of the water. Wagner obtained a solution for this shape as well as the velocity field, and determined the force of the water on the board as

$$P = \frac{\frac{1}{2}\pi c\rho U U_n [1 + X_0/c]^2 [1 - (X_0/c)^{-2}]}{(x_0/c - 1)(X_0/c - c/X_0 + 2\log X_0/c)}, \tag{4}$$

where $X_0 = x_0 + (x_0^2 - 1)^{\frac{1}{2}}$ and the other symbols are defined in figure 8, in which t denotes time.

In the range $1{\cdot}5 < x_0/c < 5$, (4) may be approximated by

$$P = \tfrac{1}{2}\pi c\rho U_n \frac{U}{x_0/c - 1}(0{\cdot}4 + 1{\cdot}53\, x_0/c) \tag{5}$$

to within an error of not more than 1·5 %. Because it is a convenient place to show it, the pressure distribution on the board is sketched qualitatively in figure 8, in order to point out that at small incidence the splash is very thin and therefore the stagnation point is close to the leading edge of the wetted area. It also shows that the flow under the board is everywhere in a favourable pressure gradient, so that the boundary layer may be expected to be very thin.

While Wagner's assumption that the board incidence is small usually holds in the case of surfboard flows, the assumption that $F \to \infty$ needs to be examined. The effect of gravity on two-dimensional planing flows is shown well in Sedov's (1965) summary of his own and other work in the Russian literature (notably by Gurevich and Chaplygin). As an example of the results of this work, figure 9 shows the force coefficient divided by the incidence, the location of the centre of pressure and the fractional contribution of the wave and splash drag plotted against F for steady planing of a flat plate at small incidence. All these quantities asymptotically approach constants as $F \to \infty$. Above $F = 2{\cdot}5$ (F being based on the wetted length $2c$) C_P/β changes only by 15 % of its asymptotic value, the location of the centre of pressure does not change, and the wave drag represents less than 25 % of the splash drag. This wave drag is, of course, that due to gravity waves, the Weber number having been considered zero. The ratio of wave drag to splash drag is independent of β.

A very detailed experimental investigation of boards planing under asymmetric conditions at $F \simeq 10$ on a flat horizontal water surface was made by

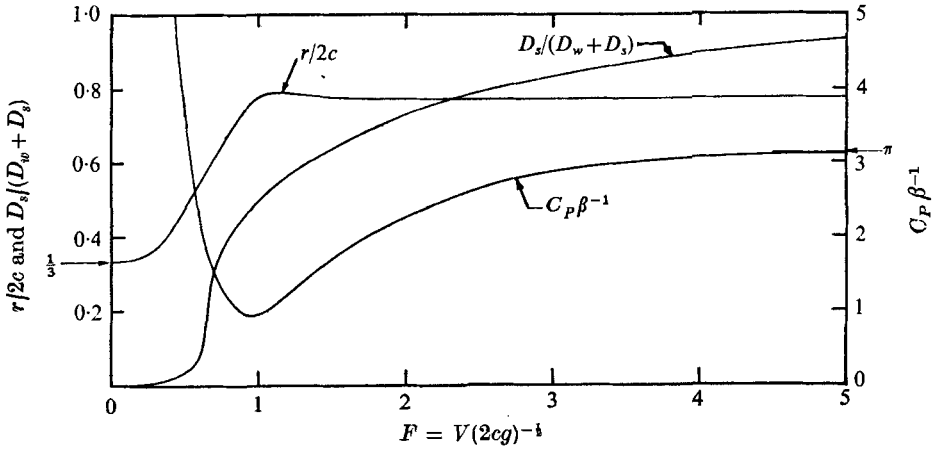

FIGURE 9. Effect of Froude number (from Sedov 1965). D_s = splash drag, D_w = wave drag, r = distance of the centre of pressure from the trailing edge.

Savitsky, Prowse & Lueders (1958), who measured forces and moments with a balance. Their results essentially confirm Wagner's (1932) predictions where these are appropriate. They also demonstrate that scale effects are not detectable by comparing their results, taken with a 2 in. beam model, with those of Weinstein & Kapryan (1953), which were obtained with a 4 in. beam model.

An experimental investigation in which surfboards were tested on a stationary wave (with normal orientation to the flow) was made by Paine (1974). Of particular interest in this project were stepped-bottom boards and boards with discontinuous rocker curve slope.

4.3. *A straight-sided plane surfboard riding on a plane wave face*

Consider the problem of figure 8 and its solution by Wagner (1932) for inviscid flow and $F \to \infty$, $W \to 0$. This problem is plane and essentially unsteady, i.e. it may not be made steady by any Galilean transformation. However, if the plate is inclined slightly, so that the trailing edge makes a small angle with the water surface, an analogous three-dimensional problem is generated, which is no longer essentially unsteady, because an observer moving with the velocity of the point where the trailing edge intersects the water surface sees it as steady. This change from an essentially unsteady n-dimensional problem to an analogous steady $(n+1)$-dimensional one has been a successful trick in various fields in fluid mechanics. In fact the same technique has been used in § 3 to relate the steady three-dimensional breaking wave to a two-dimensional unsteady plunging breaker. The time in the flow of figure 8 is replaced in the analogous three-dimensional steady problem by the distance along the trailing edge. A sketch of the three-dimensional steady flow is shown in figure 10. The fact that the flow in figure 8 is centrally similar makes the flow field in figure 10 conical, all properties of the flow being constant along rays through the similarity centre for the case of a semi-infinite board. Note that the analogy takes account of the induced velocity field due to the trailing vortex system on the starboard side of

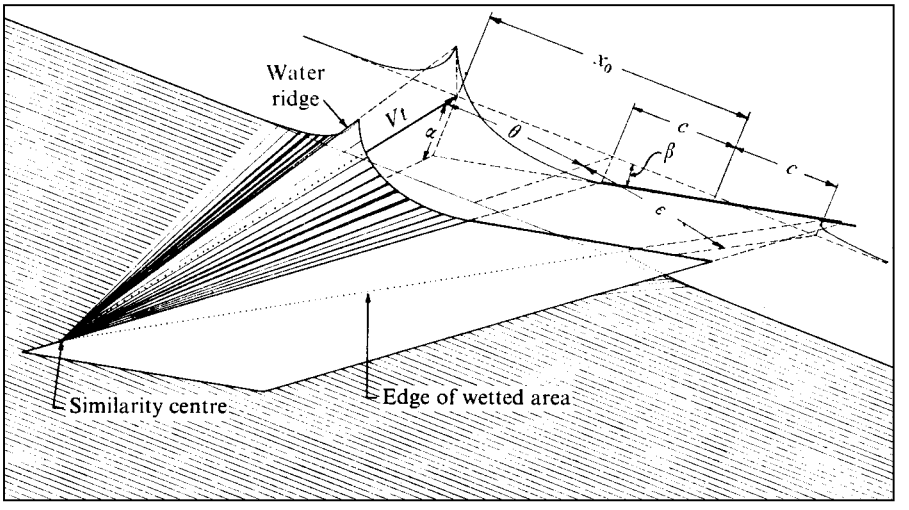

FIGURE 10. Relating Wagner's problem (figure 8) to the plane surfboard on a plane wave face.

the board in figure 10, which corresponds to the vortex sheet of the two-dimensional unsteady case.

When $F \to \infty$, gravity becomes unimportant and there is no preferred orientation of the undisturbed water surface. The water surface in figure 10 may therefore be thought of as sloping to the horizontal at a finite angle by rotating the figure through this angle. To indicate this, figure 10 is drawn with the water surface obliquely across the page. Viewed in this frame, the undisturbed water surface resembles a wave face, being inclined to the horizontal, with the water moving uphill. The attitude of the board and the flow around it are qualitatively similar to the surfboard situation, as can be seen by comparing them with the photograph in figure 11 (plate 2), although the surfing situation is more complicated for a number of reasons. These are that F and W are finite, the undisturbed water surface is curved, the board edge and bottom surface are curved, and the leading edge of the wetted surface usually emerges on the leading side of the board rather than at the tail. An interesting effect due to a combination of finite F and water-surface curvature is the gradual overturning of the water ridge evident in figure 11 (plate 2).

The flow in figure 10 is defined by the three angles α, θ and β. The velocities U and U_n in the corresponding two-dimensional unsteady problem (see figure 8) are

$$U = V\theta, \quad U_n = V\alpha. \tag{6}$$

In order to calculate the load per unit length from (5) it is necessary to determine x_0/c by finding the shape of the deformed surface in order to locate the leading edge of the wetted area. Alternatively, if the angle ϵ is known, (5) may be expressed in the form

$$P = \tfrac{1}{4}\pi c\rho V^2 \alpha\epsilon\,(1{\cdot}93 + 3{\cdot}06\theta/\epsilon). \tag{7}$$

This may be regarded as the lift per unit length of the board, and the total lift of a board of wetted length d may be determined from $L = \int_0^d P\, d(Vt)$. Since $c = \frac{1}{2}\epsilon Vt$, this gives

$$L = \tfrac{1}{2}\rho V^2 \tfrac{1}{2}\epsilon d^2 \tfrac{1}{4}\pi\epsilon\alpha\,(1{\cdot}93 + 3{\cdot}06\theta/\epsilon). \tag{8}$$

It should be pointed out that in the derivation of (8) the facts that the board is finite and that the variation of lift along its length affects the applicability of Wagner's two-dimensional result have been neglected. However, (8) can be tested in the experimental results of Savitsky *et al.* (1958). The cases selected for this purpose are those with a triangular wetted area and cover the range $10° \leqslant \theta \leqslant 20°$, $35° \leqslant \epsilon \leqslant 55°$ at $\alpha = 6°$ and $F \approx 12$. The comparison shows that (8) (with $\sin\epsilon$ replacing ϵ) agrees with Savitsky's results within $\pm 15\,\%$.

L is the component normal to the undisturbed water surface of the total force exerted by the water on the board. The component parallel to the undisturbed water surface is not necessarily parallel to the undisturbed streamline in this three-dimensional flow (see figure 17).

Since the centre of pressure for each element of the board lies at $0{\cdot}44c$ from the leading edge of the wetted area (see figure 9) the centre of pressure for the total board may be expected to lie approximately at a point $\frac{2}{3}d$ from the similarity centre on the line $x = x_0 + 0{\cdot}56c$.

4.4 *The model surfboards and their performance*

It is part of the experience of every experimenter that the multitude of small effects neglected in the process of arriving at the theoretical prediction of a phenomenon usually cause its experimental verification to be a lengthy process during which stray effects have to be eliminated carefully in order to achieve the right balance of conditions. It may be imagined, therefore, how pleased and excited we were when the first model board was able to ride the model wave unsupported. The board was made 18 cm long of balsa wood and weighted with plasticine according to the scaling law $P \propto d^3$ to make up the correct total weight to represent 70 kg of board and rider at 1/12 scale. It was able to ride the wave despite the scale effects (R and W) and despite the inability of the plasticine weight to correct for the effect of the fluctuations of the water surface. One of the benefits of this result is that it obviates the necessity for building a force balance. This would be a very difficult task in any case, because the board would have to be held by the balance in just the right position and attitude to match the water surface. Because of the fluctuations in the water surface the problem would be even more difficult. As it is, the forces normal and parallel to the water surface may be measured simply by recording the slope of the water surface and resolving the total weight in the appropriate directions. A photograph of the board on the wave is shown in figure 12 (plate 2). This photograph again shows the rolling over of the water ridge downstream of the board. It also shows the nylon fishing line (10 lb strength) attached to the bow of the model for safety. This is quite flexible and transmits only an extremely small force to the model. It appears particularly thick in the light of the flash in this photograph.

In order to test the effect of some simple board-shape parameters, while also being able to measure the position of the leading edge of the wetted area, nine model surfboards were made of Perspex with three different bottom shapes and three different planforms. The three photographs of figure 13(*a*) (plate 3) show the planforms and the bottom shapes. The latter are made clear by projecting a Ronchi grating onto the boards at an oblique angle from a distance large compared with the board length, so that the fringes on the boards (which were temporarily painted white for this purpose) represent contours. The convex 'vee', flat and concave bottom shapes are shown with the 'vee' tail, narrow roundtail and pintail planforms. Figure 13(*b*) (plate 3) shows one of the boards from the side indicating the centre-line curve, or rocker, and the fin shape and position. These parameters were made as nearly as possible the same among the nine boards. Figure 13(*b*) gives an indication of the height difference between the contours of figure 13(*a*). The Perspex boards were made as light as possible, by shaping only the bottom surface correctly, the top being made flat, in order to reduce the ratio of board mass to rider mass, which is much larger in the model case (20·2 g: 20·2 g) than in the prototype case (4 kg: 66 kg). Consequently the scaled pitch and yaw moments of inertia are much larger and the centre of mass is lower in the model system. It also means that only steady-state surfing and translationally accelerating situations can be modelled.

To show that the experimental flow underneath the board does resemble the flat, straight-sided board situation at high F, figure 14 (plate 4) shows a transparent board viewed from above. On the starboard side of the board the water ridge can be seen to be preceded by some capillary waves and the leading edge of the wetted area is quite clearly discernible through the board. Where this edge emerges from under the board on the port side, the splash can be seen as a fold in the water surface. Behind this point the flow is, of course, no longer like that in figure 10. By making some approximate measurements of the quantities in (8) from this and a side-on photograph, it is possible to estimate the lift force. With $\theta = 5°$, $\epsilon = 18°$, $d = 13$ cm (to make $\frac{1}{2}\epsilon d^2$ equal to the total wetted area), and $\alpha = 5°$, (8) gives $L = 47\,000$ dyne for the case of figure 14. This is to be compared with the measured value of 37 000 dyne. In view of the inaccuracies in the procedure for estimating L and of the differences between the model surfboard flow and the idealization of figure 10, this discrepancy is remarkably small. The fact that the estimate is within a factor of 2 of the measurement supports the view that figure 10 gives the right qualitative description of the front part of the steady surfboard flow.

The position of the centre of mass of the surfboard plus load is marked as a cross in figure 14. This lies further to starboard than one would expect from the prediction of the centre-of-pressure position (see § 4.3). The reason for this is the lift force on the fin, which acts transversely across the board to starboard at a point below the board, thus tending to tip the board over towards port. The board lift and weight forces have to form a couple to counteract this torque. The function of the fin is to prevent excessive side-slip, that is to maintain the angle θ small. Without it, the board's most stable attitude would be close to broadside on. The effective incidence of the fin is very difficult to determine

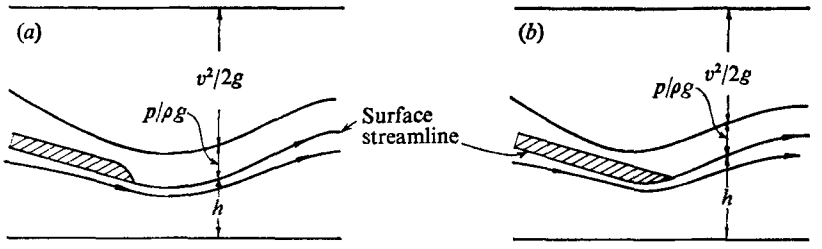

FIGURE 15. The pressure under (*a*) sharp-edged and (*b*) round-edged boards as qualitatively obtained from applying the continuity and Bernoulli equation to the guessed streamtube area, giving a lower pressure for (*b*).

because of the three-dimensional nature of the flow under the board. Under some circumstances the fin may keep the board so close to the undisturbed streamline direction that θ is negative. The model of figure 10 would then become invalid.

A very important part of the surfboard shape is the sharpness of those parts of the board edge at which the flow leaves the board (see also Paine 1974). The reason for this may be illustrated by considering a rounded and sharp trailing edge of a two-dimensional planing board in the light of the Bernoulli equation. Figure 15 presents these two situations showing a surface streamline and the qualitative behaviour of the pressure, velocity and height along it. The area change along the stream tube demands a velocity change, which together with the height change determines the pressure change. This shows that the pressure under the board in figure 15 (*a*) is lower than that in figure 15 (*b*), with a resulting decrease in lift. The suction under the tail of the board associated with a rounded edge (or with excessive rocker) enables surfboard riders with long, heavy boards to perform the trick of 'hanging ten', that is, standing at the front of the board (in front of the wetted area) with all toes protruding over the edge.

4.5. *Estimates of the drag and scale effects*

Since α is not zero, the total force due to the pressure on the board bottom has a drag component. The splash drag may be estimated from Wagner's theory. Both of these drag components may be expected to be the same for the model and prototype situation provided that the board attitude is the same in both cases. Whether it will be or not depends, however, on the skin-friction and wave-making contributions to the drag.

To estimate the skin-friction contribution it is convenient to approximate the boundary-layer flow on the board by a two-dimensional model with a linearly decreasing pressure (see figure 8). The Falkner–Skan solutions apply to this idealization of the flow if the boundary layer is laminar, giving an average skin-friction coefficient of

$$C_f = 1{\cdot}37\,(\nu/Vd)^{\frac{1}{2}}, \tag{9}$$

where $\nu = \mu/\rho$. To estimate the transition-point position, the minimum critical Reynolds number for instability is used, in accordance with the results of Granville (see Schlichting 1965, figure 16.21), the free-stream turbulence level

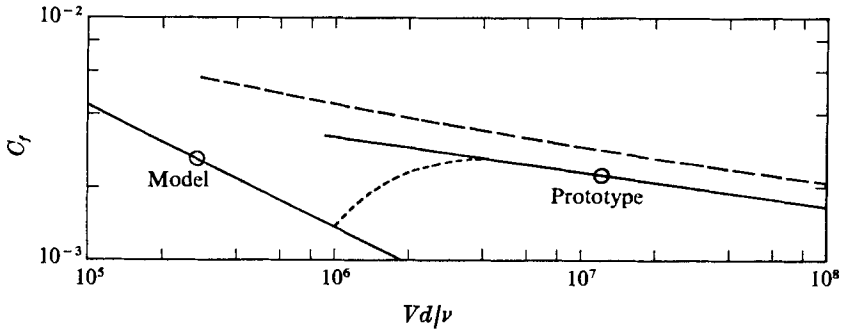

FIGURE 16. The average skin-friction coefficient on a plate with linearly decreasing pressure. – – –, zero pressure gradient.

	Model	Prototype
Lift coefficient	0·06	0·06
Pressure drag coefficient	0·0063	0·0063
Splash drag coefficient	0·0017	0·0017
Gravity-wave d.c.	0·0004	0·0004
Capillary-wave d.c.	0·0004	0
Skin-friction d.c. (board)	0·0026	0·0023
Skin-friction d.c. (fin)	0·0007	0·0002
Total estimated drag coefficient	0·0121	0·0109
Displacement thickness (cm)	0·02	0·1

TABLE 1

being very high. For the linear pressure distribution (corresponding to a Pohlhausen parameter of 5·5) Schlichting's figure 17.3 gives the minimum critical Reynolds number (here converted to distance along the plate s) of $Vs/\nu = 10^6$. Adopting this as the transition Reynolds number, it is clear that the boundary layer on the model boards ($Vd/\nu = 2{\cdot}7 \times 10^5$) is laminar. The displacement thickness of the boundary layer is approximately 0·02 cm at the end of the plate.

For the prototype board, $Vd/\nu = 1{\cdot}1 \times 10^7$. Most of the boundary layer is therefore turbulent, and can be estimated by the method outlined by Schlichting (1965, § XXII.3). This method yields the turbulent skin-friction curve shown in figure 16, in which the flat-plate skin-friction curve is included for comparison. Also shown is the laminar skin-friction curve as given by (10). The boundary-layer displacement thickness at the end of the plate is 0·1 cm according to this estimate. The model and prototype points shown on figure 16 indicate that the average skin-friction coefficients for model and prototype may be expected to be nearly the same. The fact that the boundary layer is not turbulent in the model flow, while modifying the very small dimensionless boundary-layer thickness, actually helps the modelling, by maintaining the drag coefficient more nearly equal to the prototype value.

The gravity-wave-making contribution to the drag may be estimated from figure 9 as being 25 % of the splash drag at the operating Froude number of 2·5.

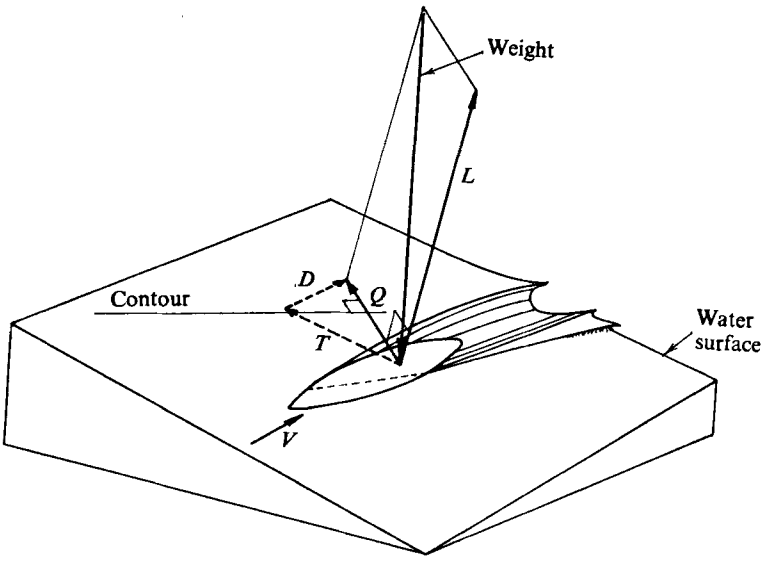

FIGURE 17. The forces exerted by the water on the board balance the weight. Q, T and D are in the plane of the water surface, L is perpendicular to it. Q is directed at right angles to the surface contour and D is parallel to V.

By estimating the capillary wave height at 0·05 cm and assuming that the increased pressure associated with it acts over an area equal to the wave height times the board width, a capillary-wave-making drag coefficient of 4×10^{-4} is obtained. Adding up the various contributions for model and prototype gives the results in table 1 for the case of figure 14. All force coefficients are based on the wetted area of the board A. The direction of the component of force in the plane of the water surface Q is the direction of the steepest gradient of the water surface (see figure 17). It is made up of the fin lift plus transverse force due to the asymmetry of the planing condition T and the fin drag plus board drag D. The total water-plane force coefficient $Q/\frac{1}{2}\rho V^2 A$ turns out to be 0·020 for the case of figure 14, the water surface gradient being 18° at the operating point. Only the drag component of this force is likely to be sensitive to R and W and table 1 shows that these scale effects only amount to about 10% of $D/\frac{1}{2}\rho V^2 A$. By measuring the angle between V and Q, the separate components T and D may be determined in the experiment. For the case of figure 14, this angle is 42°. Hence $T/\frac{1}{2}\rho V^2 A$ is measured at 0·015 and $D/\frac{1}{2}\rho V^2 A$ as 0·0134, indicating that the drag estimate of table 1 (in which most three-dimensional effects are neglected) is 11% low.

4.6. *Summary of force measurements and longitudinal stability*

The results for the stationary planing of the nine boards are given in table 2. The columns called nose lift and tail lift describe the rocker curve, being measured from the tangent to the centre-line of the bottom at the widest beam point. Unfortunately the nose and tail lifts did not remain constant on the Perspex boards owing to stress relaxation, and they could not be made the same

Planform	Hull	Tail lift (mm)	Nose lift (mm)	A (cm^2)	d (cm)	ϕ_f (deg)	ϕ (deg)	ψ (deg)	C_L	C_Q	C_D	ad/gq
Pintail	V	3·5	8·0	28·4	10·5	4	2·8	14·4	0·056	0·014	0·011	1·1
	Flat	2·5	9·0	28·4	9·3	4	3·5	14·4	0·056	0·014	0·011	0·8
	Concave	2·5	9·0	27·7	8·6	7	3·8	18·3	0·058	0·019	0·014	0·7
Veetail	V	2·0	8·0	25·8	8·1	5	6·0	16·8	0·061	0·018	0·013	0·5
	Flat	2·0	10·0	26·5	7·8	6	8·5	17·9	0·061	0·019	0·014	0·7
	Concave	1·5	7·0	26·3	7·6	6	4·5	17·9	0·061	0·019	0·014	1·1
Narrow	V	2·5	8·0	26·9	8·7	2	5·3	—	0·059	—	—	0·5
round	Flat	2·0	9·0	25·0	7·2	4	7·5	19·4	0·062	0·022	0·016	0·6
tail	Concave	2·0	7·0	23·9	7·1	5	6·5	14·7	0·069	0·018	0·013	0·6
Error		±0·5	±0·5	±5%	±0·1	±0·5	±1·0	±1·0	±8%	±15%	±15%	±15%

TABLE 2. Summary of measurements on model surfboards. ϕ_f is the angle between the flume wall and V in a horizontal plane. ϕ is the angle between the board centre-line and V in a horizontal plane. ψ is the maximum slope of the undisturbed water surface at the operating point. Further

$$C_L = L/\tfrac{1}{2}\rho V^2 A, \quad C_Q = Q/\tfrac{1}{2}\rho V^2 A \quad \text{and} \quad C_D = D/\tfrac{1}{2}\rho V^2 A.$$

sufficiently accurately. It is therefore difficult, particularly for the vee-tails, to draw any significant conclusions from the variations in lift, side force and drag coefficients with board shape. However, the concave boards are able to ride the wave stably at a higher point on the wave and, like the vee-bottom boards, are able to surf with less side-slip. They appear to give more lift. The last row in table 2 gives an indication of the estimated error in the tabulated quantities.

The effect of moving the centre of mass is to cause the board to accelerate approximately in the direction of the centre-of-mass shift. Thus a shift of the centre of mass a little to the wave-face side of forward causes the board to accelerate forward along the surface contour. The board acceleration is much more sensitive to transverse shifts than to longitudinal shifts. However, when the centre of mass is shifted a little back of the transverse direction towards the wave face, it climbs up the wave face and, because of the resulting reduction in lift, finds a new stable position. It is extremely difficult in the present experiments to explore the higher stable positions of the boards because the water surface choppiness causes the boards to be thrown off balance.

The longitudinal stability of the boards is determined by measuring the acceleration a resulting from a given longitudinal displacement q of the centre of mass. This is done by holding the board at its steady operating point, releasing it and timing its progress along the wave contour over a fixed distance of about one board length. The acceleration a is determined by assuming it to be constant over this distance. The stability in the form of a force per distance of centre-of-mass shift may be determined from these results. It turns out to be 2700 dyne/cm with a scatter of about $\pm 50\,\%$ among the nine boards. In dimensionless form, this may be expressed as $ad/gq \approx 0{\cdot}75$ with forward and backward acceleration.

5. Conclusions

The aims of this work, to generate a stationary, oblique breaking wave in the laboratory and to demonstrate that surfboards can be tested on such a wave, have been achieved. The first part of the work has shown that the wave provides a convenient means of studying two-dimensional breaking waves inasmuch as the three-dimensional steady oblique wave is analogous to the two-dimensional unsteady normal breaker. One of the features of such a wave, the dividing stream surface, is discussed in § 3. Such a surface would be very difficult to recognize in two-dimensional unsteady experiments because it would appear as a set of moving path lines. Apart from the effect of surface tension to round off all sharp edges on the wave, no significant scale effects are involved in modelling the wave, and Froude-number similarity is automatically satisfied.

Model surfboards can be tested with quantitative success on such a wave. They are able to ride it unsupported, so that all forces may be determined by resolving the weight in the appropriate directions. For the model tests to be more accurate than here, it would be necessary to produce a wave with less surface choppiness and to make the surfboards with more precision. The smaller fluctuations of the board would then make more accurate determinations of the

board attitude possible (e.g. using a light beam reflected from a mirror mounted on the board). The surfboard modelling is likely to suffer from significant scale effects only in the drag component of the force exerted by the water, where they are estimated to contribute about 10 %. Since the relative mass of the board is much larger in the model situation, dynamic stability measurements are not possible with the present method of model construction. However, measurements involving linear accelerations are valid, and one such measurement (of longitudinal stability) is described in § 4.6. In the present experiments only a fixed-total-weight situation is examined. A method of changing the operating point of a given board on a particular wave would be to vary the total weight. The additional parameters introduced into the problem by changing the weight would require much more extensive experiments, but this appears to be an interesting direction in which to extend them.

To test the slight evidence that a concave board has more lift than one with a flat or convex vee bottom, one of us (P.K.) has built a full-size board whose main feature is a transition from a convex vee bottom at the front (for sea-keeping ability) to concave at the tail (for steady-state high lift). Its edge has a transition from a bevelled chine at the bow to a round edge at the maximum beam point to a sharp edge towards the tail. To date, only subjective information is available on this board: those who have ridden it speak very highly of its manoeuvrability and speed.

A stationary breaking wave may, of course, also be produced at full scale, for example by placing a suitable obstacle in a fast-flowing river. Such a wave might be used for surfing for pleasure, for teaching people to ride boards or for detailed board-shape investigations. The fact that it could be ridden for hours on end, rather than only for about 30 seconds as is typical of ocean breakers, would be very attractive to the dedicated surfer.

We should like to thank Dr Keith Crook of the Department of Geology, ANU, for making the flume available for the experiments, and Mr K. C. Smith for his excellent efforts in the extensive photographic work involved in the project. The photographs of figures 4(*a*) and 11 were kindly made available by *Surfing World*. Figure 12 is reproduced from a photograph taken by Dr S. M. A. Meggitt.

REFERENCES

LAMB, H. 1932 *Hydrodynamics*, § 256. Cambridge University Press.

PAINE, M. 1974 B.E. thesis, Mech. Engng Dept., Sydney University.

SAVITSKY, D., PROWSE, R. E. & LUEDERS, D. H. 1958 *N.A.C.A. Tech. Note*, no. 4187.

SCHLICHTING, H. 1965 *Grenzschicht-Theorie*. Braun.

SEDOV, L. I. 1965 *Two-dimensional Problems in Hydrodynamics and Aerodynamics*. Interscience.

STOKER, J. J. 1957 *Water Waves*. Interscience.

WAGNER, H. 1932 *Z. angew. Math. Mech.* **12**, 193–215. (English trans. *N.A.C.A. Tech. Memo.* no. 1139.)

WEHAUSEN, J. V. & LAITONE, E. V. 1960 In *Handbuch der Physik* (ed. S. Flügge), vol. IX. Springer.

WEINSTEIN, I. & KAPRYAN, W. J. 1953 *N.A.C.A. Tech. Note*, no. 2981.

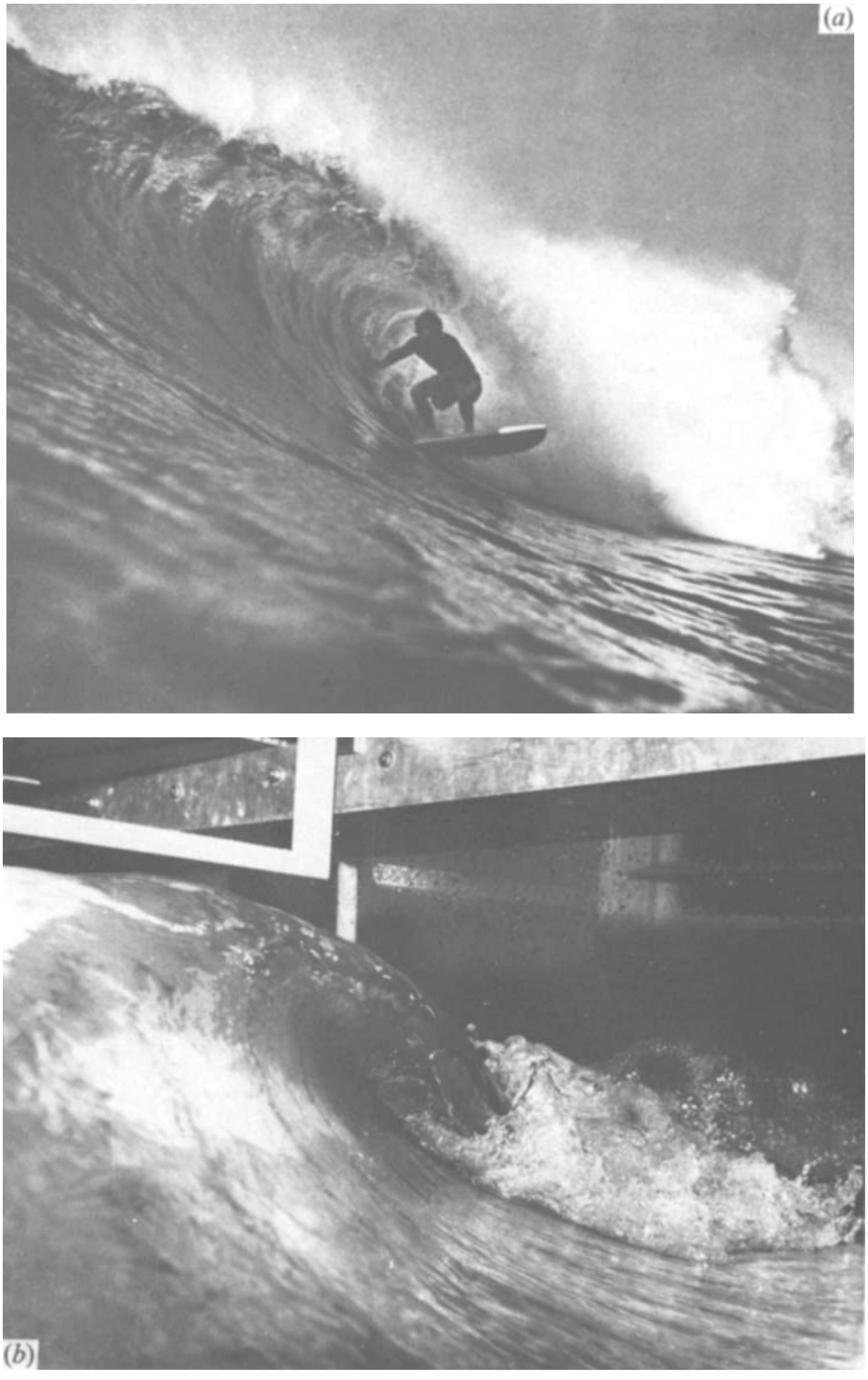

FIGURE 4. (*a*) Desirable wave shape showing a surfer in a somewhat bumpy ride. (*b*) Model wave produced in the flume.

FIGURE 11. Showing the wake of a surfboard. Note the overturning of the water ridge due to gravity and surface curvature.

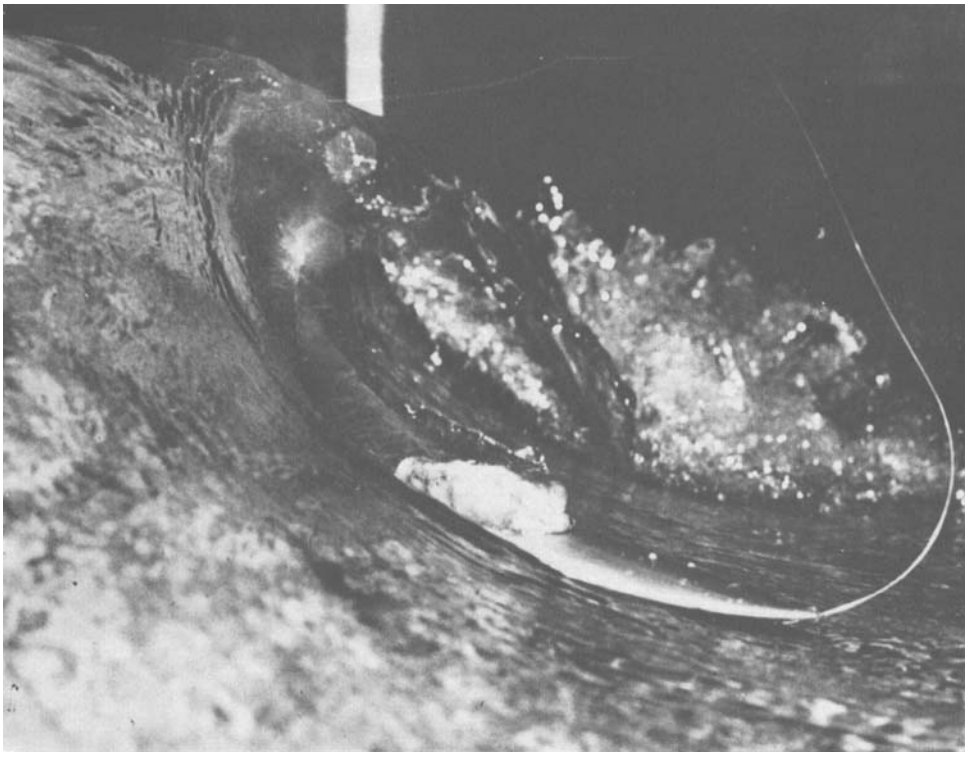

FIGURE 12. Balsa-wood surfboard model weighted with plasticine, riding the model wave. The force transmitted to the board through the nylon fishing line is negligible compared with the water forces. Note again the overturning of the water ridge behind the board.

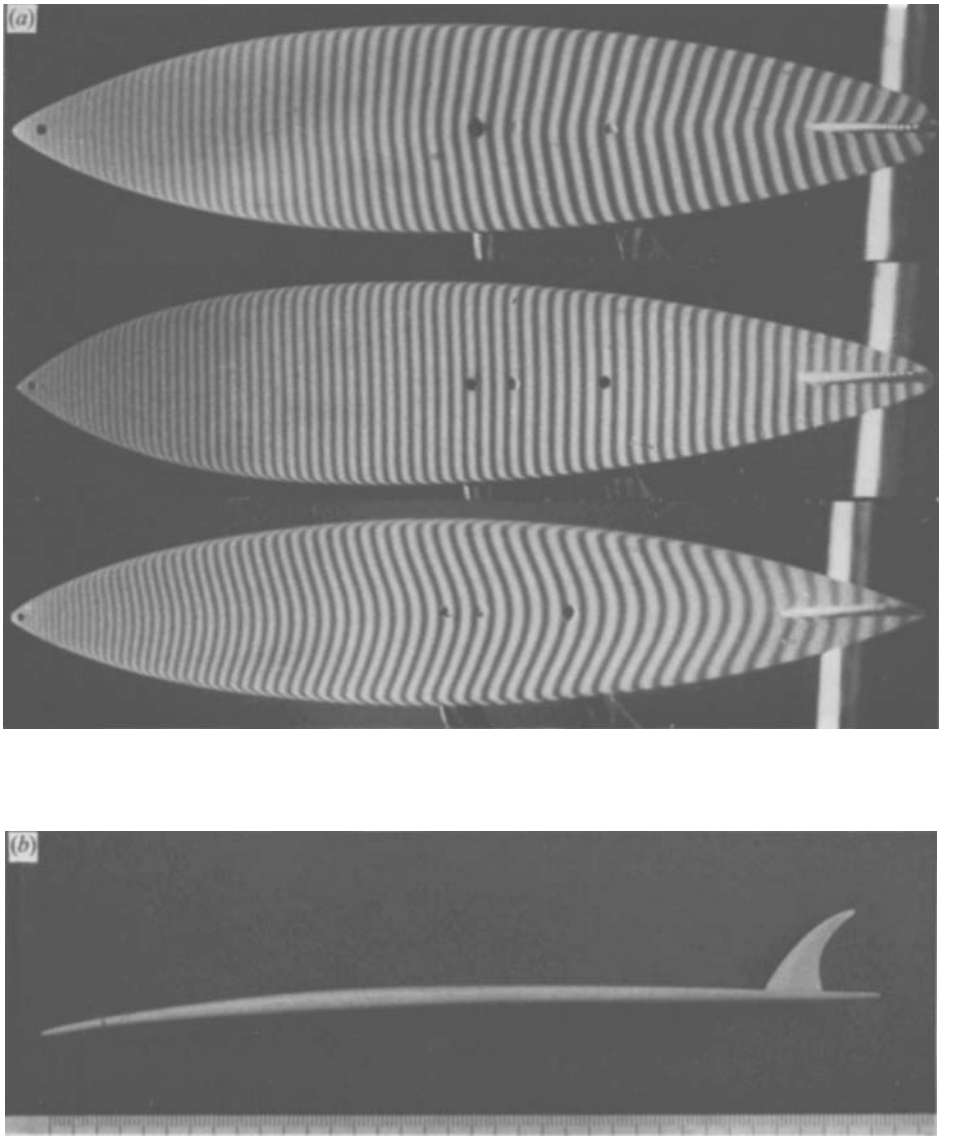

FIGURE 13. (*a*) Planforms and bottom shapes of the surfboard models. Top: convex vee-bottom, vee-tail; middle: flat bottom, narrow round tail; bottom: concave bottom, pin tail. The bottom shapes are made visible by projecting a Ronchi grating obliquely onto the boards, thus producing fringes which represent contours of height. (*b*) Side view of surfboard model showing rocker curve and fin.

FIGURE 14. Top view of transparent surfboard model riding the wave. The cross marks the centre-of-mass position. Note the leading edge of the wetted area and the starboard side capillary waves.